Electron beam analysis and sensitivity studies for the EuPRAXIA@SPARC_LAB RF injector

Journal of Physics: Conference Series **2687** (2024) 032022 doi:10.1088/1742-6596/2687/3/032022

Electron beam analysis and sensitivity studies for the EuPRAXIA@SPARC_LAB RF injector

A Giribono [1] D Alesini [1], A Bacci [4], M Bellaveglia [1], F Cardelli [1], E Chiadroni [3], A Del Dotto [1], L Faillace [1], M Ferrario[1], A Gallo [1], A Ghigo[1], G Giannetti[2], A Mostacci [3], M Opromolla [1], V Petrillo [5], L Piersanti [1], R Pompili [1], S Romeo [1], M Rossetti Conti [4], A R Rossi [4], V Shpakov [1], G J Silvi [3], C Vaccarezza [1]

[1] INFN-LNF, Via Enrico Fermi 54, 00044 Frascati, Italy
[2] Department of Information Engineering, University of Florence, Florence, Italy
[3] La Sapienza University of Rome, Rome, Italy
[4] INFN-MI, Milan, Italy
[5] University degli Studi di Milano, Milan, Italy

E-mail: anna.giribono@lnf.infn.it

,

Abstract. The interest in plasma-based accelerators as drivers of user facilities is growing worldwide thanks to their compactness and reduced costs. The EuPRAXIA@SPARC_LAB collaboration is preparing a technical design report for a multi-GeV plasma-based accelerator with outstanding electron beam quality to pilot an X-ray FEL, the most demanding in terms of beam brightness. The beam dynamics has been studied aiming to a reliable operation of the RF injector to generate a so-called comb-beam with 500 MeV energy suitable as driver of the Beam-driven Plasma Wakefield Accelerator. A case of interest is the generation of a trailing bunch with 1 GeV energy, less than 1 mm-mrad transverse emittance and up to 2 kA peak current at the undulator entrance. The comb-beam is generated through the velocity bunching technique, an RF compression tool that enables high brightness beams within relatively compact machine. Since it is based on a rotation of the beam phase space inside the external RF fields, it could be particularly sensitive to amplitude and phase jitters in the RF injector. The electron beam dynamics and the machine sensitivity to the possible jitters are presented in terms of effect on the beam quality so to provide the basis for the jitter tolerances.

1. Introduction

At EuPRAXIA@SPARC_LAB, the unique combination of an advanced high-brightness RF injector and a plasma-beam driven accelerator will drive a new multi-disciplinary user-facility [1]. The main application concerns the operation of a soft X-ray FEL driven by a 1 GeV high brightness electron beam. In details, the identified reference working point foresees the running of the RF linac in tandem with the plasma module, operated in the particle-beam driven scheme with a 200 pC driver followed by a 30 pC witness beam. The beams are generated in the photo-injector; then they are boosted in energy up to 650 MeV in the downstream linac and injected in the plasma thanks to a focusing system of permanent quadrupoles. In view of the next Technical Design Report drafting, intense beam dynamics studies are ongoing to explore very different configurations in terms of beam parameters and machine layout. This paper reports

on the beam dynamics of the described working point and on its sensitivity to jitters in the photo-injector.

2. Beam dynamics studies

Beam dynamics in the EuPRAXIA@SPARC_LAB accelerator has been studied by means of start to end simulations from the cathode up to the undulator entrance. The beam longitudinal phase space at the linac exit is mainly determined by the plasma module. In details, the driver-witness delay must be around 0.5 ps, which corresponds to half of the plasma wavelength ($\lambda_p/2$), i.e. almost 334 μm for a plasma background density of the order of $10^{16} cm^{-3}$ and the driver and witness bunches must be compressed down to 50 fs and 10 fs (FWHM), respectively. A fine tuning of witness current and beam time delay is then essential for an efficient acceleration while preserving the beam quality, mitigating the beam loading among others, in the plasma [2].

2.1. The Photo-Injector

The photo-injector consists of an RF gun, equipped with a photo-cathode laser and an emittance compensation solenoid, followed by an X-band standing wave and four S-band traveling wave accelerating structures. The first two S-band sections are surrounded by solenoids to enable the emittance compensation in case of RF longitudinal compression [3]. This layout is an updated version of the one described in [4] and results from various iterations based on beam dynamics considerations aiming to compact the machine as much as possible, to meet the longitudinal dimension of the host building, and to guarantee same time the needed beam features required from the downstream modules. The customised layout is based on the length shrinking of the second to fourth accelerating sections that allows for higher sustainable accelerating gradient, i.e. up to 35 MV/m, and for reducing the active space dedicated to the velocity bunching regime for the benefit of the overall energy boost. The first accelerating section, instead, keeps its original length so to still ensure a wide range of tunability of witness-driver delays and witness peak current, without necessarily switching-on the X-band cavity after the gun.

The beam dynamics has been studied by means of simulations performed with the TStep code [6] that takes into account the space charge effects, relevant at very low energies and the intrinsic emittance at the cathode. The witness and driver bunches have been simulated with 30k and 200k macro-particles respectively, corresponding to 30 pC and 200 pC. The photo-cathode laser has been shaped in order to provide at the cathode the witness pulse preceding the driver of 4.8 ps. The witness and driver have gaussian longitudinal distributions with 290 fs rms length and uniform transverse distribution of 175 and 350 μm rms size respectively. The driver spot size on the cathode has been chosen looking at the witness quality that strongly depends on the density of the beams at the overlapping point as illustrated in [4]. The gun operates with a peak field at the cathode of 120 MV/m; a slightly dephasing between the field and the beam allows to maximise the energy gain in this part. The first three S-band structures operate at almost 20 MV/m and the third one at 35 MV/m on average. The magnetic field of the solenoids are set close to the invariant envelope condition [5]. This scheme ensures at same time up to 2 kA peak current and beams closer than 0.6 ps at the plasma [7]. The following sections operate almost on crest to let the electron bunch gain the energy and freeze its phase space quality, without lowering the witness peak current. At the photo-injector exit the witness arrives 0.50 ps later than the driver with an emittance of 0.55 mm-mrad and a peak current of 1.9 kA, while the driver is 60 μm long as required by the plasma module. The Figure 1 shows the phase space distributions at the photo-injector injector exit.

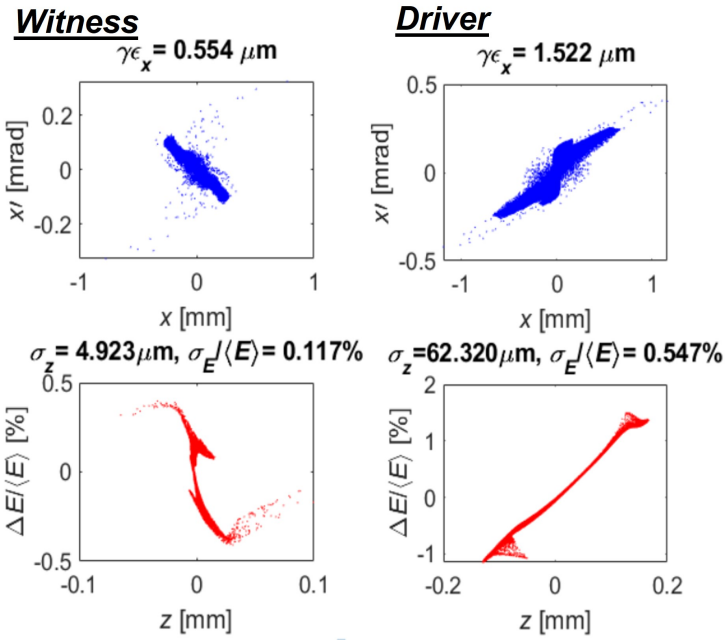

Figure 1. Witness and driver phase space distributions at the photo-injector injector exit. The beams exit the photo-injector with 126 MeV energy and are separated by 0.503 ps.

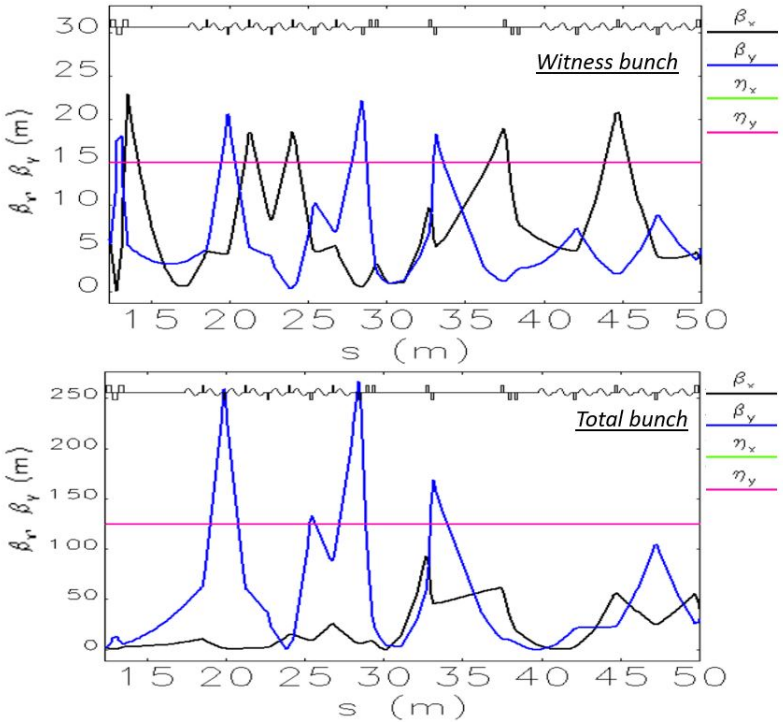

Figure 2. Evolution of the witness and overall beam along the X-band linac. The beam transverse size remains always smaller than the X-band irises with maximum spot size in the matching quadrupoles of the order of 0.7 mm.

2.2. The X-band Linac

The X-band RF linac, operating at 11.994 GHz, is composed of sixteen accelerating sections, a laser heater, a magnetic chicane and several matching sections of quadrupoles for transport the beam through the X-band linac and finally up to plasma entrance. The accelerating structures are 0.9 m long, consisting of 8.3 mm long cells with average iris of 3.5 mm, and can sustain average gradient up to 60 MV/m so to allow enough margin for the off-crest operation and minimize the final beam energy spread. Electron beam dynamics simulations in the booster linac have been performed with the Elegant code [8] that includes the longitudinal space charge and the coherent and incoherent synchrotron radiation effects in the bending magnets and the wakefields generated by the electron beam inside the accelerating structures. An evaluation of off-axis beam dynamics along the linac is shown in [9] and [10]. The Figure 2 reports the evolution of the Twiss parameters along the linac for the witness and the overall bunch. The beam transverse size remains always smaller than the X-band irises with maximum spot size in the matching quadrupoles of the order of 0.7 mm. The beam is then transversely focused down to 1 μm spot size thanks to a focusing system, consisting in an electro-magnet and a permanent quadrupole triplet, that has been designed to match the beam transversely at the plasma entrance with a beta function of about 1 mm at the plasma interface at the waist. The beam dynamics in this part of the machine has been simulated with TStep to take into account, and eventually mitigate, the transverse emittance and longitudinal distribution dilution due to the space charge contribution that can arise due the strong focusing of the beams.

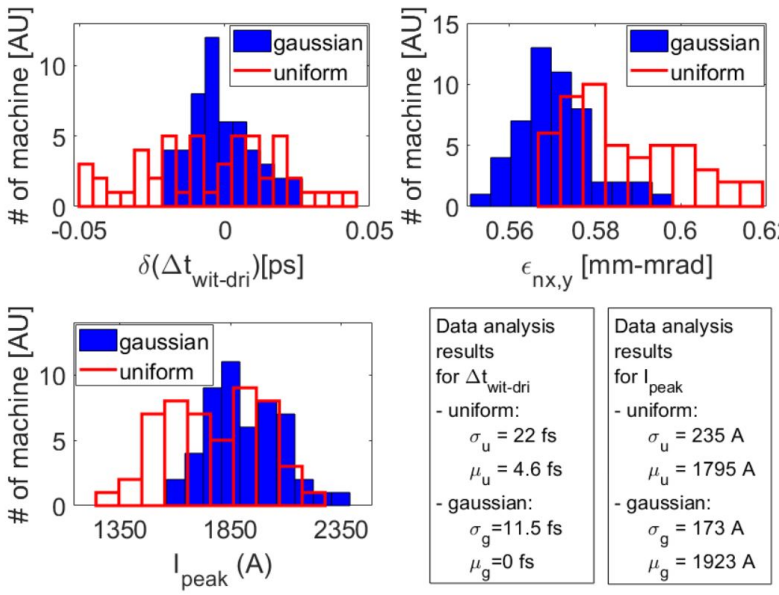

Figure 3. Jitter analysis in terms of the witness emittance and peak current and the witness-driver delay in case of all jitter as listed in 2.2 for uniform (red histograms) and gaussian (blue histograms) error distribution.

3. Machine sensitivity studies

Tolerances studies are essential in the TDR workflow and aim to actual check the robustness and reliability of the adopted working point, especially with regards to the phase stability

Table 1. Maximum values of the jitters introduced on the RF gun, accelerating cavities and photo-cathode laser system.

Parameter	Value	Units
RF Voltage [ΔV_{GUN}]	± 0.1	%
RF Phase [$\Delta\Phi_{GUN}$]	±0.1	deg
RF Voltage [$\Delta V_{Sections}$]	±0.1	%
RF Phase [$\Delta\Phi_{Sections}$]	± 0.1	deg
Charge Fluctuation [δQ]	± 2	%
Laser time of arrival [Δt]	± 0.1	ps
Laser spot size[$\delta\sigma_r$]	± 1	%

of RF elements as needed to ensure a μm scale bunch length and a fs scale precision of the time delay between the bunches, critical parameters for an efficient operation of the plasma module. The sensitivity studies have started from the photo-injector, while other systematic errors and jitters on the overall machine will be tackled later. Indeed, the photo-injector is the main responsible of the beam compression and delay definition and of jitter introduction due to the adopted velocity bunching mode. Since the RF compression strongly depends on the RF phase stability, at first the phase jitters on the accelerating cavities, gun and laser time of arrival at the cathode have been introduced one by one to determine most dangerous error contributions. Then, all jitters, except for the pointing instability at the cathode, have been introduced afterwards. Taking advantage of the experience acquired at the SPARC_LAB test facility [11], the maximum reasonable error values have been considered to face the most realistic situation (Table 2.2), trying not to count only on the best performance of the machine systems. Machine sensitivity studies have been performed on samples of 50 machine runs (due to computational limits). For each machine we have generated a tracking code input whose element errors are provided by means of the Matlab Latin Hypercube function that returns an n-by-p matrix. This matrix contains a latin hypercube sample of n machine run identifier on each of the p element errors: the n values are randomly distributed with one from each interval (0,1/n), (1/n,2/n), ..., (1-1/n,1), and they are randomly permuted. Furthermore a normal random distribution of minus and plus sign is also applied. In this way the error matrix randomly factorizes from -100% to +100% the considered error values listed in Table 2.2 for each element. The data analysis highlights that the RF phase jitter mostly impacts on the witness length and on the witness-driver delay. In details, studying the RF phase errors one by one, it turns out that the laser time of arrival and the first accelerating section are the main culprits of the jitter of the interested quantities and that the witness-driver delay linearly depends on the amplitude of the considered error. The linear trend allows for evaluating the jitter of the witness-driver delay on the basis of analytical calculation, as describe in [12], so to not rely on hundreds of multi-particle simulations. Analytical and numerical studies have shown to be in good agreement between them and indicate time delay jitter between the beams of the order of 22 fs rms in case of same power source for the first two accelerating sections (the ones involved in the compression). Further studies have demonstrated that is possible to suppress the temporal jitter quantities of the 10% if one feeds the first and second accelerating sections with uncorrelated power sources. It has to be noticed that the analysed scenario represents a worst case one with uniform distributions for the jitter listed in Table 2.2, while the reality lies on gaussian distribution errors with same maximum error values. Both analytic evaluation and simulations, performed on a sample of 50 machine runs, suggest that the temporal jitter of the

beams is almost halved if one considers a realistic gaussian distribution for the errors listed in Table 2.2. The Figure 3 reports the jitter analysis in terms of the witness emittance and peak current and the witness-driver delay in case of all jitter as listed in Table 2.2 for uniform (red histograms) and gaussian (blue histograms) error distributions. The analysis shows in the worst case scenario a worsening of the emittance and of the peak current of maximum 10% even if still remaining in specification. The most critical parameter is instead the witness-driver delay, that should not exceed the 10 fs rms value for a reliable operation of the plasma accelerating module.

4. Conclusions

The electron beam dynamics has been described in the EuPRAXIA@SPARC_LAB machine with an insight on the working point chosen as reference on the basis of start to end simulations, from the cathode up to the undulator entrance. Studies on the machine sensitivity needed in view of the TDR has been addressed and first results on the most critical part of the RF injector, the photo-injector, has been illustrated with promising results. In the next future the robustness of the adopted working point will be completed also taking into account the beam dilution due to the wake-field in the downstream X-band linac.

Acknowledgments

This project has received funding from the European Union's Horizon 2020 Research and Innovation programme under grant agreement No 777431 and No. 653782.

References

[1] Ferrario M *et al.*, "EuPRAXIA@SPARC_LAB design study towards a compact FEL facility at LNF", *Nucl. Instrum. Methods Phys. Res. Sect. A*, vol. 909, pp. 134–138, Nov. 2018. doi:10.1016/j.nima.2018.01.094

[2] Romeo S *et al.*, "Numerical studies for EuPRAXIA@SPARC_LAB plasma beam driven working point ", presented at the IPAC'23, Venice, Italy, May 2023, paper TUPL132, this conference.

[3] Ferrario M *et al.*, "Experimental demonstration of emittance compensation with velocity bunching", *Phys. Rev. Lett.*, vol. 104, p. 054801, Feb. 2010. doi:10.1103/PhysRevLett.104.054801

[4] Giribono A *et al.*, "EuPRAXIA@SPARC_LAB: the high-brightness RF photo-injector layout proposal", *Nucl. Instrum. Methods Phys. Res. Sect. A*, vol. 909, pp. 282–285, Nov. 2018. doi:10.1016/j.nima.2018.03.009

[5] Serafini L and Rosenzweig J B, "Envelope analysis of intense relativistic quasilaminar beams in rf photoinjectors: A theory of emittance compensation", *Phys. Rev. E*, vol. 55, pp. 7565–7590, Feb. 1997. 10.1103/PhysRevE.55.7565

[6] Young L M and Billen J, "The particle tracking code PARMELA", in *Proc. PAC'03*, Portland, OR, USA, May 2003, paper FPAG029, pp. 3521–3523.

[7] Silvi G J *et al.*, "Beam dynamics optimization of EuPRAXIA@SPARC_LAB RF injector ", presented at the IPAC'23, Venice, Italy, May 2023, paper WEPA040, this conference.

[8] Borland M, "ELEGANT: A flexible SDDS-compliant code for accelerator simulation", presented at the *6th International Computational Accelerator Physics Conference (ICAP 2000)*, Darmstadt, Germany, September 2000, paper LS-287.

[9] Vaccarezza C *et al.*, "EUPRAXIA@SPARC_LAB: Beam dynamics studies for the X-band linac", *Nucl. Instrum. Methods Phys. Res. Sect. A*, vol. 909, pp. 314–4317, Nov. 2018. doi.org/10.1016/j.nima.2018.01.100

[10] Bosco F *et al.*, "Advanced studies for the dynamics of high brightness electron beams with the code MILES ", presented at the IPAC'23, Venice, Italy, May 2023, paper WEPL190, this conference.

[11] Pompili R *et al.*, "Recent results at SPARC_LAB", *Nucl. Instrum. Methods Phys. Res. Sect. A*, vol. 909, pp. 139–144, Nov. 2018. doi.10.1016/j.nima.2018.01.071

[12] Pompili R *et al.*, "Femtosecond timing-jitter between photo-cathode laser and ultra-short electron bunches by means of hybrid compression", *New J. Phys.*, vol. 18, pp. 083033, Aug. 2016. doi.org/10.1088/1367-2630/18/8/083033